

Non-Abelian spin-orbit gauge: Persistent spin helix and quantum square ring

Son-Hsien Chen* and Ching-Ray Chang

Department of Physics, National Taiwan University, Taipei 10617, Taiwan

We re-express the Rashba and Dresselhaus interactions as non-Abelian spin-orbit gauges and provide a new perspective in understanding the persistent spin helix [Phys. Rev. Lett. **97**, 236601 (2006)]. A spin-orbit interacting system can be transformed into a free electron gas in the equal-strength Rashba-Dresselhaus [001] linear model, the Dresselhaus [110] linear model, and a one-dimensional system. A general tight-binding Hamiltonian for non-uniform spin-orbit interactions and hoppings along arbitrary directions, within the framework of finite difference method, is obtained. As an application based on this Hamiltonian, a quantum square ring in contact with two ideal leads is found to exhibit four states, insulating, spin-filtering, spin-flipping, and spin-keeping states.

PACS numbers: 72.25.Dc, 85.75.-d, 73.21.Hb, 03.65.Vf

I. INTRODUCTION

The spin-orbit (SO) interaction interests scientists not only for its wide applications in spintronics devices, but also for its profound fundamental spin physics. As frequently discussed, the Rashba spin-orbit (RSO) interaction and Dresselhaus spin-orbit (DSO) interaction exist in two-dimensional electron gas (2DEG) made of semiconductor heterostructures. The former, with strength adjustable via the gate voltage[1, 2] results from the inversion asymmetry of the structure[3], while the latter is due to lack of bulk inversion symmetry.[4, 5] The SO coupling acts as an effective magnetic field[6] and thus rotates spin. In general, this field depends on the electron momentum, while in the two cases, Rashba-Dresselhaus [001] (linear) model of equal-strength RSO and DSO couplings and the Dresselhaus [110] (linear) model, it is independent of the direction of momentum. Therefore, in such two special cases, the precession angle depends only on the traveling distance but not on the moving-direction of the electron. Accordingly, the electron precesses as a helix and the precession pattern, i.e. the spin configuration, is persistent against any momentum-dependent (but spin-independent) scatterings. The so-called persistent spin helix[7, 8] (PSH) is thus resulted.

Earlier study by Hatano *et. al.*[9] shows that SO interactions can be regarded as non-Abelian SO or $SU(2)$ gauges $\mathbf{A}^{\text{SO}} = (A_x^{\text{SO}}, A_y^{\text{SO}}, 0)$ which impose spin-dependent phases on the traveling electron. By further adjusting the strength of the RSO coupling and of the magnetic field and neglecting the DSO coupling, they achieve a perfect spin-filtering ring in which one spin component gains destructive interference while the other gains constructive one. Nevertheless, the more realistic case of the coexistence of RSO and DSO interactions has not been considered.

In this paper, we consider the RSO- and DSO-

interacting system subject to an external magnetic field. We will point out that, even with the coexistence of RSO and DSO, the SO interactions and magnetic field can as well all be regarded as gauges. To obtain the discrete (in space) tight-binding (TB) model, we employ the finite-difference[10] (FD) method and analogize the $SU(2)$ gauge with $U(1)$ gauge, i.e., analogize the SO gauge with the magnetic gauge. The condition of performing this analogy will be specified. We justify this SO-interacting TB model by checking its consistency with a previously proposed one.[11] Utilizing these gauges, we show that: (i) For continuous Hamiltonian, the predicted PSH[7, 8] can be understood easily from the perspective of gauge transformation. (ii) For discrete TB Hamiltonian, a square ring functions as a versatile device with four states, insulating, spin-filtering,[9] spin-flipping and spin-keeping states.

This paper is organized as follows. Both of Secs. II and III are divided into two parts which focus respectively on the continuous and discrete cases. The Hamiltonian is studied for the continuous one in Sec. II A and the discrete one in Sec. II B. Applications are also given in Secs. III A and III B for both cases. The Rashba-Dresselhaus [001] linear Hamiltonian is focused throughout this article, except in Sec. III B where we consider also the Dresselhaus [110] linear model to demonstrate the PSH. We summarize in Sec. IV.

II. SPIN-ORBIT GAUGE IN THE RASHBA-DRESSELHAUS [001] LINEAR HAMILTONIAN

We study, in this section, the single-particle Rashba-Dresselhaus [001] linear Hamiltonian. In Sec. II A, we introduce the RSO and DSO interactions and show that they can be expressed as gauges. To make this Hamiltonian numerically treatable, we discretize it in Sec. II B by considering a TB model for the free-electron system subject to an external magnetic field.

*Electronic address: d92222006@ntu.edu.tw

A. Continuous case

Spin-orbit interactions in the 2DEG (x - y plane) are commonly modeled by taking into account the lowest order (linear) in momentum \mathbf{p} . Consider a heterostructure grown along the [001] direction. The corresponding single-particle Hamiltonian, together with the kinetic energy and the magnetic gauge \mathbf{A}^B , reads

$$H = \frac{\mathbf{\Pi}^2}{2m} + \frac{\alpha}{\hbar} (\Pi_y \sigma_x - \Pi_x \sigma_y) + \frac{\beta}{\hbar} (\Pi_x \sigma_x - \Pi_y \sigma_y), \quad (1)$$

with α and β denoting the RSO- and DSO- coupling strengths, respectively. The magnetic field \mathbf{B} is introduced by the kinetic momentum $\mathbf{\Pi} = \mathbf{p} - e\mathbf{A}^B/c$. Since Eq. (1) has the highest order being quadratic in $\mathbf{\Pi}$, one can always properly shift the operator $\mathbf{\Pi}$ so that the linear term disappears. By doing so, the SO gauge,

$$\mathbf{A}^{\text{SO}} = (A_x, A_y) \equiv \frac{mc}{e\hbar} (\alpha\sigma_y - \beta\sigma_x, -\alpha\sigma_x + \beta\sigma_y), \quad (2)$$

due to the presence of SO interactions, and magnetic gauge \mathbf{A}^B can be treated on an unified ground. The Hamiltonian Eq. (1) thus becomes

$$H = \frac{1}{2m} \left(\mathbf{\Pi} - \frac{e}{c} \mathbf{A}^{\text{SO}} \right)^2 - VI_s \quad (3)$$

$$= \frac{1}{2m} \left(\mathbf{p} - \frac{e}{c} \mathbf{A} \right)^2 - VI_s,$$

with the constant potential $V = (m/\hbar^2) (\alpha^2 + \beta^2)$. The algebra of Pauli matrices $\sigma_i^2 = 1$ and $\{\sigma_i, \sigma_j\} = 2\delta_{ij}$ with $i, j \in \{x, y, z\}$ is used in arriving at Eq. (3). The unified spin-dependent gauge $\mathbf{A} = \mathbf{A}^B I_s + \mathbf{A}^{\text{SO}}$ now is no longer a scalar, and its components, in general, are non-commutative,

$$[A_x, A_y] = 2i \times \left(\frac{mc}{e\hbar} \right)^2 (\alpha^2 - \beta^2) \sigma_z. \quad (4)$$

Although the presence of the non-Abelian gauge field \mathbf{A}^{SO} , usually referred to as the Yang-Mills field,[13] makes the usual scalar gauge formalism incapable and thus complicates the problem, the exception to the commutation Eq. (4) is clearly seen when RSO and DSO couplings are of equal strengths $|\alpha| = |\beta|$. In addition, for the one-dimensional system, since only one component of the gauge \mathbf{A}^{SO} will be introduced via Eq. (3), the non-commutative relation Eq. (4) will not necessarily be confronted. In Sec. III A, we will show that both cases can be transformed into the free electron gas. In particular, for $|\alpha| = |\beta|$ in Rashba-Dresselhaus [001] model, this transformation is a gauge transformation that simplifies the physical description of the PSH.[7, 8]

B. Discrete case: Tight-binding model

Conventional TB model[14] is based on the real crystal structure. Assuming that each electron orbital is localized around its associated nuclei, all spatial interactions

involving more than three nuclei centers can thus be neglected. In other words, considering only the nearest-neighbor hopping $t_{\mathbf{m}\sigma\mathbf{m}'\sigma'}$, from site \mathbf{m}' with spin σ' to site \mathbf{m} with spin σ , will be sufficient and is the case in the present work. The Hamiltonian can therefore be represented in the form

$$\mathcal{H}^{\text{TB}} = \sum_{\mathbf{m}\sigma} u_{\mathbf{m}\sigma} c_{\mathbf{m}\sigma}^\dagger c_{\mathbf{m}\sigma} + \sum_{\langle \mathbf{m}, \mathbf{m}' \rangle_{\sigma\sigma'}} t_{\mathbf{m}\sigma, \mathbf{m}'\sigma'} c_{\mathbf{m}\sigma}^\dagger c_{\mathbf{m}'\sigma'}, \quad (5)$$

with the on-site energy $u_{\mathbf{m}\sigma}$ tunable by the gate voltage, and the fermion creation (annihilation) operators being denoted by $c_{\mathbf{m}\sigma}$ ($c_{\mathbf{m}\sigma}^\dagger$), obeying $\{c_{\mathbf{m}\sigma}, c_{\mathbf{m}'\sigma'}^\dagger\} = 1$.

On the other hand, the FD method[10] approximates differentiations by discretizing variables. For example, the differentiation $p_x \psi(x)$, from the momentum operator p_x , is replaced with $-i\hbar(\psi_{x+a} - \psi_{x-a})/a \cong -i\hbar d\psi(x)/dx$. Clearly, this approximation is valid only when the wave function $\psi(x)$ varies slowly over one lattice constant a , or under the condition $a \ll 1$. Physically, this is the case in which only electrons near the band bottom, where $p = \hbar k$ is small, enter our problems. Despite such a restriction, this method is still quite general and powerful since it can deal with any single-particle Hamiltonian by a matrix form so that the problem can be solved by numerical method. Even though the FD method is based on different physical assumptions than the conventional TB model, the single-particle Hamiltonian can always be expressed in the form[10] of Eq. (5). In particular, it allows us to make the continuous Hamiltonian Eq. (1) a connection to the discrete SO-interacting TB model.

Consider the free-electron system,

$$H^{\text{free}} = \frac{\mathbf{\Pi}^2}{2m}. \quad (6)$$

The TB Hamiltonian corresponding to Eq. (6) reads[10],

$$\mathcal{H}^{\text{free}} = \sum_{\mathbf{m}\sigma} c_{\mathbf{m}\sigma}^\dagger c_{\mathbf{m}\sigma} u_{\mathbf{m}\sigma}^{\text{free}} + \sum_{\langle \mathbf{m}, \mathbf{m}' \rangle_{\sigma\sigma'}} t_{\mathbf{m}\sigma, \mathbf{m}'\sigma'}^{\text{free}} c_{\mathbf{m}\sigma}^\dagger c_{\mathbf{m}'\sigma'}. \quad (7)$$

Each dimension contributes the quantity $2t_0 I_s$ to the on-site energy, and in a square lattice we therefore have

$$u_{\mathbf{m}}^{\text{free}} = 4t_0 I_s, \quad (8)$$

with $u_{\mathbf{m}\sigma}^{\text{free}} = \langle \sigma | u_{\mathbf{m}}^{\text{free}} | \sigma \rangle$, the hopping strength defined as $t_0 = \hbar^2/2ma^2$, and the spin identity matrix denoted by I_s . The magnetic gauge \mathbf{A}^B is introduced as a phase factor in the hopping matrix

$$t_{\mathbf{m}, \mathbf{m}'}^{\text{free}} = -t_0 \exp \left[\frac{ie}{\hbar c} \mathbf{A}^B \cdot (\mathbf{m} - \mathbf{m}') \right] I_s, \quad (9)$$

with $t_{\mathbf{m}\sigma, \mathbf{m}'\sigma'}^{\text{free}} = \langle \sigma | t_{\mathbf{m}, \mathbf{m}'}^{\text{free}} | \sigma' \rangle$. We note that the phase acquired by an electron hopping from one site to another

only by a gauge $(e/c)\mathbf{A}^{\text{SO}}$. This suggests to consider the transformation,

$$\begin{aligned} U(\mathbf{r}) \Pi U^\dagger(\mathbf{r}) &= \Pi + \frac{ie}{\hbar c} [\mathbf{A}^{\text{SO}} \cdot \mathbf{r}, \Pi] \\ &+ \frac{1}{2} \left(\frac{ie}{\hbar c} \right)^2 [\mathbf{A}^{\text{SO}} \cdot \mathbf{r}, [\mathbf{A}^{\text{SO}} \cdot \mathbf{r}, \Pi]] + \dots, \end{aligned} \quad (18)$$

with $[\mathbf{A}^{\text{SO}} \cdot \mathbf{r}, \Pi] = i\hbar \mathbf{A}^{\text{SO}}$. Unsatisfactorily, due to the non-commutability $[A_x^{\text{SO}}, A_y^{\text{SO}}] \neq 0$, the higher order terms in Eq. (18), in general, do not vanish, leading to $U(\mathbf{r}) h U^\dagger(\mathbf{r}) \neq H$.

Exceptionally, in the equal-strength case $|\alpha| = |\beta|$, A_x^{SO} and A_y^{SO} follow the scalar algebra $A_x^{\text{SO}} A_y^{\text{SO}} = A_y^{\text{SO}} A_x^{\text{SO}}$, and hence we obtain $U(\mathbf{r}) \Pi U^\dagger(\mathbf{r}) = \Pi - e/c \mathbf{A}^{\text{SO}}$, or the gauge transformation,

$$U^\dagger(\mathbf{r}) H U(\mathbf{r}) = h. \quad (19)$$

As a result, the free electron gas h in Eq. (17) and the SO-interacting electron gas H in Eq. (3) share the same eigenenergies E_k . Their corresponding eigenfunctions, denoted by $\psi_{E_k}(\mathbf{r}) \chi_s^{\text{free}}$ and $\Psi_{E_k}(\mathbf{r}) \chi_s^{\text{SO}}$, respectively, differ from each other only by a phase factor from the 2×2 matrix $U(\mathbf{r})$, namely, $\Psi_{E_k}(\mathbf{r}) \chi_s^{\text{SO}} = U(\mathbf{r}) \psi_{E_k}(\mathbf{r}) \chi_s^{\text{free}}$. Moreover, any wave function is constructed by a superposition of the eigenfunctions, so that for any given wave function $\psi(\mathbf{r}) \chi_s^{\text{free}}$ in h , the corresponding wave function in H is $U(\mathbf{r}) \psi(\mathbf{r}) \chi_s^{\text{free}}$. Below, we show that the physical description of the PSH in the SO interacting system can be easily understood by this correspondence.

Consider first an injected electron in system h , described by $\psi_{\text{inj}}(\mathbf{r}) \chi_{\text{inj}} = [\sum_{\mathbf{k}} C_{\mathbf{k}} \psi_{E_{\mathbf{k}}}(\mathbf{r})] \chi_{\text{inj}}$, with the initial spin state χ_{inj} and the weight factor $C_{\mathbf{k}}$. Clearly, without any spin-dependent mechanisms, this electron shall retain its spin state χ_{inj} as it traverses the sample. Now, import \mathbf{A}^{SO} . This corresponds to turning on $U(\mathbf{r})$ so that the electron wave function, in the SO-interacting system H , undergoes a gauge transformation of $U(\mathbf{r})$,

$$U(\mathbf{r}) \psi_{\text{inj}}(\mathbf{r}) \chi_{\text{inj}} = \sum_{\mathbf{k}} C_{\mathbf{k}} \psi_{E_{\mathbf{k}}}(\mathbf{r}) U(\mathbf{r}) \chi_{\text{inj}}. \quad (20)$$

Accordingly, the spin polarization of the electron varies spatially according to $U(\mathbf{r}) \chi_{\text{inj}}$. Using Eqs. (16) and (2), with $\alpha = \beta$, we find that

$$\begin{aligned} U(\mathbf{r})|_{\alpha=\beta} &= \exp \left[-\alpha \frac{i2m}{\hbar^2} \sigma_{(1,-1)} r_{(1,1)} \right] \\ &= \exp \left[-i \frac{\hbar \sigma_{(1,-1)}/2}{\hbar} \theta_{\text{PSH}}^+ \right], \end{aligned} \quad (21)$$

with $\sigma_{(1,-1)} \equiv (\sigma_x, \sigma_y) \cdot (1, -1)/\sqrt{2}$ is actually the spin rotation operator, with rotation axis along $(1, -1)$ and

the precession angle $\theta_{\text{PSH}}^+ \equiv (4\alpha m/\hbar^2) r_{(1,1)}$ depending on the distance $r_{(1,1)} \equiv \mathbf{r} \cdot (1, 1)/\sqrt{2}$ along $(1, 1)$ [cf. Fig 2(b) in Ref. 8].

Similarly, for $\alpha = -\beta$, we have

$$U(\mathbf{r})|_{\alpha=-\beta} = \exp \left[-i \frac{\hbar \sigma_{(1,1)}/2}{\hbar} \theta_{\text{PSH}}^- \right], \quad (22)$$

corresponding to a rotation axis along $(1, 1)$ and a precession angle $\theta_{\text{PSH}}^- = (4\alpha m/\hbar^2) r_{(-1,1)}$ with $r_{(-1,1)} \equiv \mathbf{r} \cdot (-1, 1)/\sqrt{2}$. This is precisely the PSH with precession length,

$$L_P = \frac{\hbar^2 \pi}{2m\alpha}, \quad (23)$$

for spin to rotate θ_{PSH}^+ or $\theta_{\text{PSH}}^- = 2\pi$. Obviously, the PSH is robust against any spin-independent mechanisms for $U^\dagger(\mathbf{r}) V_p(\mathbf{r}) U(\mathbf{r}) = V_p(\mathbf{r})$ which holds for any potential of the form $V_p(\mathbf{r}) \propto I_s$, including the finite-size confinement due to spin-independent boundaries. In particular, the presence of \mathbf{A}^B , which determines the actual form of $\psi_{E_k}(\mathbf{r})$, clearly does not affect the PSH. This is reasonable since \mathbf{A}^B contributes only a spin-independent phase to the electron wavefunction due to the absence of the Zeeman term, and therefore does not vary the spin polarization. Inclusion of the Zeeman term requires further generalization, which is beyond the scope of the present discussion.

A similar calculation can also apply to the DSO [110] linear model,

$$H_{[110]} = \frac{p_x^2 + p_y^2}{2m} - \frac{2\beta}{\hbar} p_x \sigma_z, \quad (24)$$

with the gauge $\mathbf{A}_{[110]}^{\text{SO}} = (A_{x[110]}, A_{y[110]}, 0) \equiv (2\beta \sigma_z, 0, 0) mc/e\hbar$. Due to $[A_{x[110]}, A_{y[110]}] = 0$, we also have here the PSH described by

$$U(\mathbf{r})_{[110]} = \exp \left(-i \frac{\hbar \sigma_z/2}{\hbar} \theta_{\text{PSH}} \right), \quad (25)$$

with $\theta_{\text{PSH}} = -4m\beta x/\hbar^2$ [cf. Fig. 2(d) in Ref. 8].

We further point out here that the one-dimensional SO-interacting system (with any values of α and β), also possesses the applicability of this transformation. For example, consider a one-dimensional (along \mathbf{e}_n direction) SO-interacting conductor. Since the degrees of freedom of orthogonal directions are frozen, only $\Pi_n \equiv \Pi \cdot \mathbf{e}_n$ and $A_n^{\text{SO}} \equiv \mathbf{A}^{\text{SO}} \cdot \mathbf{e}_n$ are relevant to our problem and appear in Eq. (3). The system can now be described by $H^{1\text{D}} = [\Pi_n - (e/c) A_n^{\text{SO}}]^2 / (2m) - V^{1\text{D}}$, with $V^{1\text{D}}$ being a constant potential and the non-commutability Eq. (4) is not encountered. Following procedure similar to those above, we arrive again at the transformation $U^{1\text{D}\dagger}(r_n) H^{1\text{D}} U^{1\text{D}}(r_n) = h^{1\text{D}} = \Pi_n^2 / 2m - V^{1\text{D}}$, with $U^{1\text{D}}(r_n) = \exp[(ie/\hbar c) A_n^{\text{SO}} \cdot r_n]$ with $r_n \equiv \mathbf{r} \cdot \mathbf{e}_n$.

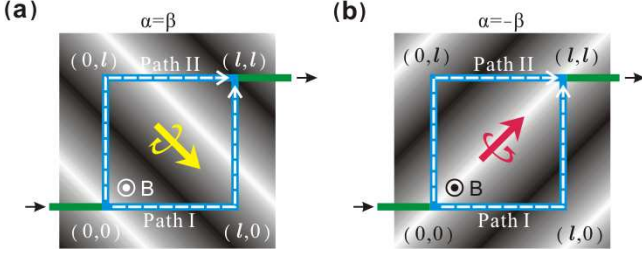


FIG. 1: (Color online) The square ring cornering at $(0,0)$, $(l,0)$, (l,l) and $(0,l)$, in contact with two leads. Magnetic field $\mathbf{B} = B\mathbf{e}_z$ is locally applied at the center of the ring. Electrons are injected from the left lead, interfered via path I and path II, and then transmitted to the right lead. The background shading represents the helix precession angle. From white to black, the electron precesses by π . The rotation axes are specified by the arrows at the centers of the rings for (a) $\alpha = \beta$ and (b) $\alpha = -\beta$.

B. Discrete case: Four states in the quantum square ring

Using the TB Hamiltonian of Eq. (14), we investigate, in this section, the square ring interferometer[9] (see Fig. 1) under the interactions of the magnetic field, DSO and RSO couplings. The transmission coefficients $T_{\sigma'\sigma}$, with incoming (outgoing) spin denoted by $\sigma(\sigma')$, depends on the interplay among the phases due to the RSO, DSO interactions and the external field. Based on different values of the magnetic field B , the Rashba coefficient α , and Dresselhaus coefficient β , four states in this setup: “perfect” insulating, spin-filtering,[9, 15, 16] spin-flipping, and spin-keeping states, will be identified. When electrons are injected into the ring, the spin-insulating ring blocks both up and down spin channels, the spin-filtering ring blocks only one of the spin channels, the spin-flipping ring flips the spins of the injected electrons, while the spin-keeping ring keeps the injected spin configuration unaltered. It is worth mentioning that these four states are valid for any range of the injected energy E as the term “perfect” stands for.

Consider a square ring (see Fig. 1) described by \mathcal{H} in Eq. (14), with width l and cornering at $\mathbf{m} = (0,0)$, $(l,0)$, (l,l) , and $(0,l)$. The magnetic field $\mathbf{B} = B\mathbf{e}_z$ penetrating this ring is applied only locally so that the Zeeman term does not emerge. Two ideal leads contact the ring at the positions $(0,0)$ and (l,l) . For brevity, and without loss of generality, we choose the on-site energy in both leads and the ring to be zero. The self-energy[10] $\Sigma(E) = (E - i\sqrt{4t_0^2 - E^2})(c_{(0,0)}^\dagger c_{(0,0)} + c_{(l,l)}^\dagger c_{(l,l)})/2$ is generated due to the presence of the leads. The transmission coefficients are computed by

$$T_{\sigma'\sigma} = \langle (l,l); \sigma' | \frac{\sqrt{4t_0^2 - E^2}}{E - \mathcal{H} - \Sigma(E)} | (0,0); \sigma \rangle, \quad (26)$$

with the incoming (from left lead) spin σ and outgoing

(to the right lead) spin σ' states denoted as $|(0,0); \sigma\rangle$ and $|(l,l); \sigma'\rangle$, respectively. The interference between the bottom-right path I $\equiv (0,0) \rightarrow (l,0) \rightarrow (l,l)$ and the left-top path II $\equiv (0,0) \rightarrow (0,l) \rightarrow (l,l)$ is determined by the phase, circling the ring, of the form $U_{\text{phase}} = U_{\text{II}}^\dagger U_{\text{I}} = [U_{(l,l) \leftarrow (0,l)} U_{(0,l) \leftarrow (0,0)}]^\dagger U_{(l,l) \leftarrow (l,0)} U_{(l,0) \leftarrow (0,0)} = U_{(0,0) \leftarrow (0,l)} U_{(0,l) \leftarrow (l,l)} U_{(l,l) \leftarrow (l,0)} U_{(l,0) \leftarrow (0,0)}$ with $U_{\mathbf{m}' \leftarrow \mathbf{m}} \equiv \exp[(ie/c\hbar)\mathbf{A} \cdot (\mathbf{m} - \mathbf{m}')] and $\mathbf{A} = \mathbf{A}^B + \mathbf{A}^{\text{SO}}$ accounting for the magnetic gauge $\mathbf{A}^B = (-By, Bx, 0)/2$ and the SO gauge Eq. (2). Explicitly, in the square ring, we obtain the 2 by 2 matrix$

$$U_{\text{phase}} = e^{i\phi^B} e^{i\frac{m_l}{\hbar^2}(\alpha\sigma_x - \beta\sigma_y)} e^{-i\frac{m_l}{\hbar^2}(\alpha\sigma_y - \beta\sigma_x)} \times e^{-i\frac{m_l}{\hbar^2}(\alpha\sigma_x - \beta\sigma_y)} e^{i\frac{m_l}{\hbar^2}(\alpha\sigma_y - \beta\sigma_x)}, \quad (27)$$

corresponding to the magnetic flux $\phi^B = (e/c\hbar)Bl^2$. Denote the general spin-up and -down along the direction with the polar angle $\theta \in [0, \pi]$ and azimuthal angle $\phi \in [0, 2\pi]$, as $\uparrow_{[\theta, \phi]}$ and $\downarrow_{[\theta, \phi]}$ respectively, i.e.,

$$\uparrow_{[\theta, \phi]} = \begin{pmatrix} e^{-i\phi/2} \cos \frac{\theta}{2} \\ e^{i\phi/2} \sin \frac{\theta}{2} \end{pmatrix}. \quad (28)$$

Strictly speaking, in the arbitrary $\uparrow_{[\theta, \phi]}$ and $\downarrow_{[\theta, \phi]}$ axes, U_{phase} does not give us the meaning of “phase”, since it is in general a non-diagonal matrix, while in the diagonal axes with $D U_{\text{phase}} D^\dagger = \Lambda$, defining the tilted up $|\tilde{\uparrow}\rangle$ (down $|\tilde{\downarrow}\rangle$) spin as $|\tilde{\uparrow}\rangle = D|\uparrow_{[0,0]}\rangle$ ($|\tilde{\downarrow}\rangle = D|\downarrow_{[0,0]}\rangle$), the circled phase $\phi_{\tilde{\uparrow}}$ acquired by $|\tilde{\uparrow}\rangle$ ($|\tilde{\downarrow}\rangle$) electron can be read off via the eigenvalues of U_{phase} ,

$$\Lambda = \begin{pmatrix} e^{i\phi_{\tilde{\uparrow}}} & 0 \\ 0 & e^{i\phi_{\tilde{\downarrow}}} \end{pmatrix}, \quad (29)$$

with $\phi_{\tilde{\uparrow}(\tilde{\downarrow})} \equiv \phi^B + \phi_{\tilde{\uparrow}(\tilde{\downarrow})}^{\text{SO}}$ contributed from both magnetic ϕ^B and SO $\phi_{\tilde{\uparrow}(\tilde{\downarrow})}^{\text{SO}}$ phases. Consider a special case with vanishing β , $\phi^B = \pi/2$, and $\phi_{\tilde{\uparrow}(\tilde{\downarrow})}^{\text{SO}} = +(-)\pi/2$. This corresponds to the Rashba strength[9],

$$\alpha^* = \frac{\hbar^2}{ml} \sin^{-1} \left(2^{-1/4} \right). \quad (30)$$

There is, therefore, destructive interference $e^{i\phi_{\tilde{\uparrow}}} = e^{i\pi} = -1$ for $|\tilde{\uparrow}\rangle$ electrons, and constructive interference $e^{i\phi_{\tilde{\downarrow}}} = e^{i0} = 1$ for $|\tilde{\downarrow}\rangle$ electrons. The spin-filtering ring (filtering out $|\tilde{\uparrow}\rangle$) is thus achieved in this case. We now numerically analyze the SO phase $\phi_{\tilde{\uparrow}(\tilde{\downarrow})}^{\text{SO}}$ and the transmission coefficients $T_{\sigma'\sigma}$ in Eq. (26).

In Figs. 2(a) and 2(b), we plot the tilted-spin-up phase $\phi_{\tilde{\uparrow}}^{\text{SO}}$ and down phase $\phi_{\tilde{\downarrow}}^{\text{SO}}$ as functions of the Rashba

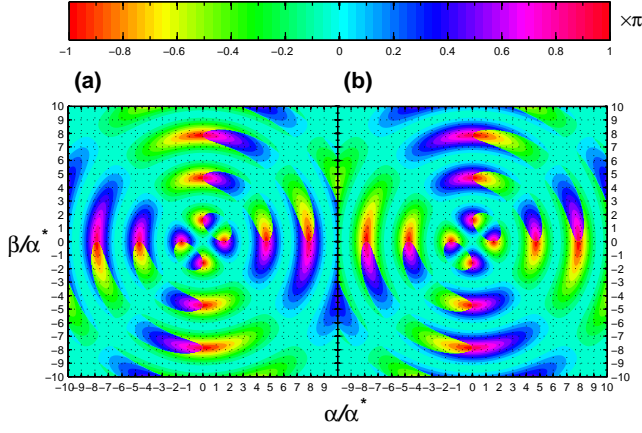


FIG. 2: (Color online) Spin-orbit phases in (a) ϕ_{\uparrow}^{SO} and (b) ϕ_{\downarrow}^{SO} as functions of α/α^* and β/α^* for the square ring patterned in the Rashba-Dresselhaus [001] 2DEG.

α/α^* and Dresselhaus β/α^* interaction strengths, with α^* defined in Eq. (30). Since $U_{\text{phase}}(\phi_B \rightarrow 0)$ in Eq. (27) is a rotation in the $SU(2)$ group, we have $\det[U_{\text{phase}}(\phi_B \rightarrow 0)] = \det \Lambda = 1$, yielding $\phi_{\uparrow}^{SO} = -\phi_{\downarrow}^{SO}$ which is clearly seen in Fig. 2. Notice that the SO phases are symmetric[17] (unchanged) under the replacement $(\alpha, \beta) \rightarrow (-\alpha, -\beta)$ but anti-symmetric (different by a sign) under $(\alpha, \beta) \rightarrow (\beta, \alpha)$. For $|\alpha| = |\beta|$, $U_{\text{phase}}(\phi_B \rightarrow 0, |\alpha| \rightarrow |\beta|) = I_s$ gives zero $\phi_{\uparrow(\downarrow)}^{SO}$. Moreover, in the vicinity of the circles $R_s = \sqrt{(\alpha^2 + \beta^2)/\alpha^{*2}} = s\pi$, $s = 0, 1, 2, \dots$, we have small SO phases $\phi_{\uparrow(\downarrow)}^{SO} \approx 0$. Between these circles are the bands where the SO phases $\phi_{\uparrow(\downarrow)}^{SO}$ oscillate at $R_{s+1/2}$ with a full period 2π within each quadrant. The fine structure inside the bands clearly shows discontinuities of $\phi_{\uparrow(\downarrow)}^{SO}$ [see, for example, the boundaries between $\phi_{\uparrow(\downarrow)}^{SO} \approx 0.4\pi$ (blue/dark) and $\phi_{\uparrow(\downarrow)}^{SO} \approx -0.4\pi$ (green/light)]. In particular, the parameter proposed for a spin filter,[9] $(\alpha, \beta)/\alpha^* = \pm 1 \times (1, 0)$, corresponding to $\phi_{\uparrow(\downarrow)}^{SO} = +(-)\pi/2$, is quite unstable. Interestingly, the presence of β does help one to move $\phi_{\uparrow(\downarrow)}^{SO}$ away from these discontinuities and makes spin filter therefore experimentally more accessible, for example, $(\alpha, \beta)/\alpha^* \cong \pm 1 \times (4.55, -1.8)$ in the second band ($\approx R_{3/2}$).

Figure 3 plots the transmission coefficients $T_{\sigma'\sigma}$, with $\sigma, \sigma' = \{\uparrow, \downarrow\}$, as functions of the injection energy E . Obviously, for any $|\alpha| = |\beta|$ with $\phi^B = (2n+1)\pi$ and $n \in \text{integer}$, the ring is completely destructive for electron spins of any directions, namely, $\phi_{\uparrow[\theta, \phi]} = \phi_{\downarrow[\theta, \phi]} = (2n+1)\pi$. We thus have the insulating state in Fig. 3(a). For the spin-filtering state in Fig. 3(b), we take the values $(\alpha, \beta)/\alpha^* = \pm 1 \times (0, 1)$ and $\phi^B = (4n+1)\pi/2$ which contribute to the \uparrow and \downarrow spins with the construc-

tive $\phi_{\uparrow} = 2n\pi$ and destructive $\phi_{\downarrow} = (2n+1)\pi$ phases. As a response to the anti-symmetric property of the $\phi_{\uparrow(\downarrow)}$ mentioned above, the indices \uparrow and \downarrow in the transmission coefficients are swapped if we interchange α and β , i.e., choose the values $(\alpha, \beta)/\alpha^* = \pm 1 \times (1, 0)$ as used in Ref. 9.

Here the destructive interference means that the outgoing channel is blocked. So far we have not utilized any relation between the incoming and outgoing spin states, which are correlated with each other by the spin precession, for example, the PSH, which yields the spin-flipping ring in Fig. 3(c) and spin-keeping ring in Fig. 3(d). We now focus on the case of $|\alpha| = |\beta|$. Without loss of generality, assume $\alpha > 0$ for simplicity. Due to $U_{\text{phase}}(|\alpha| \rightarrow |\beta|) \propto I_s$, the phases are now merely determined by the magnetic gauge and become spin-independent, i.e. $\phi^B = \phi_{\uparrow[\theta, \phi]} = \phi_{\downarrow[\theta, \phi]}$. As a result, the interference and the precession are decoupled in the PSH, and are governed separately by the magnetic and the SO gauges.

In one of the equal-strength case, namely, $\alpha = \beta$, we have, according to Eq. (21), the PSH pattern shown in Fig. 1(a). The condition $\sqrt{2}l = L_P(2s+1)/2$, with L_P defined in Eq. (23), or equivalently

$$\alpha = \beta = \frac{(2s+1)\pi\hbar^2}{4\sqrt{2}lm}, \quad (31)$$

rotate any injected spin $\uparrow_{[\theta, \pi/4]}$ (or $\downarrow_{[\theta, \pi/4]}$) along the $x = y$ plane, by the angle $\theta_{\text{PSH}}^+ = \pi(2s+1)$. For example, the sketch in Fig. 1(a) is the case with $\theta_{\text{PSH}}^+ = 3\pi$. As a result, after passing through the ring, $\uparrow_{[\theta, \pi/4]}$ is flipped to $\downarrow_{[\theta, \pi/4]}$ (or $\downarrow_{[\theta, \pi/4]}$ to $\uparrow_{[\theta, \pi/4]}$). This represents the spin-flipping ring. Indeed, under the condition (31), and with $B = 0$, our numerical result in Fig. 3(c) suggests the spin-flipping state by showing vanishing $T_{\uparrow_{[\theta, \pi/4]}\uparrow_{[\theta, \pi/4]}}$ and $T_{\downarrow_{[\theta, \pi/4]}\downarrow_{[\theta, \pi/4]}}$ but non-vanishing $T_{\uparrow_{[\theta, \pi/4]}\downarrow_{[\theta, \pi/4]}}$ and $T_{\downarrow_{[\theta, \pi/4]}\uparrow_{[\theta, \pi/4]}}$.

In the other equal-strength case, $\alpha = -\beta$, we have, according to Eq. (22), the PSH pattern shown in Fig. 1(b). Therefore, as long as the ring retains its square shape, injected spin of arbitrary direction remains in its original configuration due to the zero precession angle $\theta_{\text{PSH}}^- = 0$. One thus arrives at the spin-keeping ring in accord with Fig. 3(d) which predicts such a state by showing vanishing $T_{\uparrow_{[\theta, \phi]}\downarrow_{[\theta, \phi]}}$ and $T_{\downarrow_{[\theta, \phi]}\uparrow_{[\theta, \phi]}}$. Note that although Figs. 3(c) and 3(d) are plotted for the special case $B = 0$, the features of spin-flipping and spin-keeping are robust against magnetic field since they result from precession rather than phase change.

IV. SUMMARY

In the limit Eq. (11), the approximation Eq. (10) suggests that the $SU(2)$ or SO phases can be treated as $U(1)$

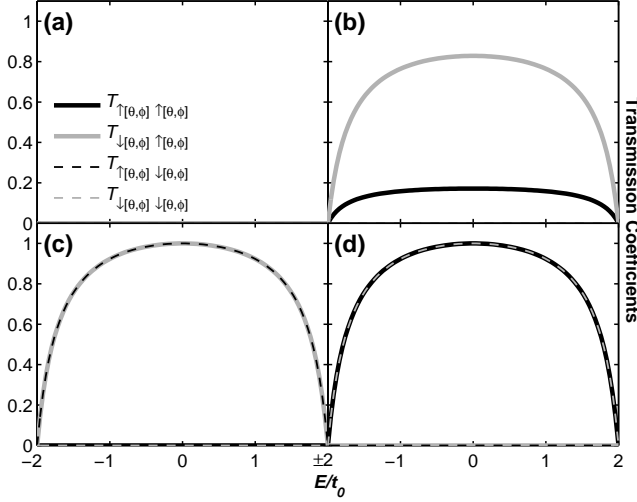


FIG. 3: Transmission coefficients $T_{\uparrow[\theta,\phi]\uparrow[\theta,\phi]}$ (black solid lines), $T_{\downarrow[\theta,\phi]\uparrow[\theta,\phi]}$ (gray solid lines), $T_{\uparrow[\theta,\phi]\downarrow[\theta,\phi]}$ (black dashed lines), $T_{\downarrow[\theta,\phi]\downarrow[\theta,\phi]}$ (gray dashed lines) as functions of energy E . In the insulating state (a) and the spin-keeping state (d), the up spin $\uparrow_{[\theta,\phi]}$ is defined by Eq. (28), for any $\theta \in [0, \pi]$ and $\phi \in [0, 2\pi]$. In the spin-filtering state (b), up-spin is defined in the tilted axes mentioned in Sec. III B, i.e., $\uparrow_{[\theta,\phi]} \equiv \hat{\uparrow}$, whereas in the spin-flipping state (c), it is defined in any directions lying in the $x = y$ plane, i.e. $\uparrow_{[\theta,\phi]} \equiv \uparrow_{[\theta,\pi/4]}$.

phases. We have justified the SO-interacting TB model, established from this analogy, with the one previously given in Ref. 11. The PSH, initially obtained from a global $SU(2)$ transformation,[7] is revisited here by performing a local gauge transformation. As an application of the geometry of the PSH pattern, we consider a square ring in contact with two ideal leads. This setup is found to be a versatile spintronics device performing four types of functions in which spins are insulated, filtered, flipped or kept (in polarization). The former two are due to phase change, while the latter two are due to spin precession and newly proposed here. The SO phases in the presence of both Rashba and Dresselhaus SO couplings are also analyzed. In particular, the SO phases, as functions of the two SO couplings, exhibit high symmetries and show discontinuities. Our numerical results on transmission coefficients confirm with theoretical predictions on the PSH and thus suggest a four state device.

Acknowledgments

One of the authors (S.H.C.) thanks Ming-Hao Liu for valuable discussions and suggestions. This work is supported by the Republic of China National Science Council Grant No. 95-2112-M-002-044-MY3.

-
- [1] J. Nitta, T. Akazaki, H. Takayanagi, and T. Enoki, Phys. Rev. Lett. **78**, 1335 (1997).
 - [2] B. Das, D.C. Miller, S. Datta, R. Reifenberger, W.P. Hong, P.K. Bhattacharya, J. Singh, and M. Jaffe, Phys. Rev. B **39**, R1411 (1989).
 - [3] E.I. Rashba, Sov. Phys. Solid State **2**, 1109 (1960).
 - [4] G. Dresselhaus, Phys. Rev. **100**, 580 (1955).
 - [5] G. Lommer, F. Malcher, and U. Rössler, Phys. Rev. B **32**, R6965 (1985); Yu. A. Bychkov and E. I. Rashba, in *Proceedings of the 17th International Conference on Physics of Semiconductors, San Francisco, 1984* (Springer, New York, 1985), p. 321; M. I. D'yakonov and V. Y. Kachorovskii, Sov. Phys. Semicond. **20**, 110 (1986).
 - [6] I. Žutić, J. Fabian, and S. Das Sarma, Rev. Mod. Phys. **76**, 323 (2004).
 - [7] B. Andrei Bernevig, J. Orenstein, and S. C. Zhang, Phys. Rev. Lett. **97**, 236601 (2006).
 - [8] Ming-Hao Liu, Kuo-Wei Chen, Son-Hsien Chen, and Ching-Ray Chang, Phys. Rev. B **74**, 235322 (2006).
 - [9] N. Hatano, R. Shirasaki, and H. Nakamura, Phys. Rev. A **75**, 032107 (2007).
 - [10] S. Datta, *Electronic Transport in Mesoscopic Systems* (Cambridge University Press, Cambridge, 1995), Sec.3.5.
 - [11] B. K. Nikolic, L. P. Zârbo, and S. D. Souma, Phys. Rev. B **73**, 075303 (2006).
 - [12] Ming-Hao Liu and Ching-Ray Chang, Phys. Rev. B **74**, 195314 (2006).
 - [13] L. H. Ryder, *Quantum Field Theory* (Cambridge University Press, Cambridge, 1985), Secs. 3.5–3.6.
 - [14] G. Grosso and G. P. Parravicini, *Solid State Physics* (Academic Press, New York, 2000), Sec. 5.2.
 - [15] J. Nitta, F. E. Meijer, and H. Takayanagi, Appl. Phys. Lett. **75**, 695 (1999).
 - [16] B. Molnár, F. M. Peeters, and P. Vasilopoulos, Phys. Rev. B **69**, 155335 (2004).
 - [17] This symmetry yields $T_{\sigma'\sigma}$ unaffected when replacing α , in Hamiltonian (1) with $-\alpha$, as used in Ref. 9 where β is further dropped.